

Site Characterization for mm/submm Astronomy

Simon J. E. Radford

*National Radio Astronomy Observatory,
949 North Cherry Avenue, Tucson, AZ 85721 USA*

Abstract. At millimeter and submillimeter wavelengths, the Earth's atmosphere presents a natural limitation to the sensitivity and resolution of astronomical observations. The translucent atmosphere both decreases the signal, by attenuating incoming radiation, and increases the noise, by radiating thermally. Pressure broadened spectral lines of tropospheric molecules, primarily water vapor, are the culprits. Furthermore, inhomogeneities in the water vapor distribution cause variations in the electrical path length through the atmosphere, resulting in phase errors that degrade the sensitivity and resolution of images made with both interferometers and filled aperture telescopes.

Because atmospheric transparency and stability often show only a poor correlation, measurements of both are necessary for site characterization. Transparency is inferred from the atmospheric brightness measured with tipping radiometers, line monitors, or Fourier transform spectrometers. Atmospheric stability can be measured directly from the phase fluctuations seen by a simple interferometer observing a convenient beacon outside the atmosphere, i. e., on a geostationary satellite. Stability can also be inferred from atmospheric brightness fluctuations.

Measurements of the 225 GHz and 350 μm atmospheric transparency with functionally identical tippers at Mauna Kea, the South Pole, and Chajnantor indicate periods of excellent observing conditions at all three sites. Conditions at Chajnantor and the South Pole are better more often than at Mauna Kea. The first quartile zenith transparencies at Chajnantor and the South Pole are roughly equal.

1. Introduction

Astronomy at short millimeter and submillimeter wavelengths, say 4 mm–300 μm , is primarily the study of cool thermal sources where temperatures seldom exceed 100 K. For example, the rotational transitions of CO and other molecules, the fine structure lines of atomic carbon, and continuum radiation from optically thin dust are essential probes for the study of star formation, planet formation, late stage of stellar evolution, the chemical history and the structure of the interstellar medium, Galactic structure, and the structure, evolution, and formation of other galaxies.

At millimeter and submillimeter wavelengths, however, the atmosphere is only partially transparent. Pressure broadened transitions of atmospheric

molecules, particularly water vapor, both absorb and emit radiation. The absorption attenuates the astronomical signal and the emitted radiation adds to the inherent noise of the receiver. The signal-to-noise ratio is degraded, then, on two counts. Indeed, for a receiver approaching the quantum noise limit and an antenna with low spillover optics, atmospheric brightness can be the predominant term in the system noise.

Moreover, turbulence in the atmospheric water vapor degrades the resolution of a telescope and further reduces its sensitivity. The electrical path length through the atmosphere varies because water vapor changes the index of refraction of air. Path length differences across the aperture of an individual antenna change the position of the beam on the sky, with deleterious effects on both the calibration of the observations and the resolution of the resulting image. Path differences between different elements of an array decorrelate the signals on short time scales, reducing the measured amplitude, and introduce phase errors on long time scales that broaden the synthesized beam.

Because water vapor is the primary cause of atmospheric opacity, the best sites for millimeter and submillimeter wavelength astronomy will have exceptionally dry air. Although it depends on local climate and weather conditions, the scale height ($1/e$) of atmospheric water vapor is typically 1–2 km (e. g., Holdaway et al. 1996). So water is trapped relatively low in the atmosphere and extremely dry air can be found above high altitude sites. Atmospheric turbulence is more complicated than the overall distribution of water vapor, as it can depend strongly on local effects and topography. Generally, turbulence is lessened if the air flow over a site encounters no upstream obstructions. Because atmospheric transparency and stability often show only a poor correlation, measurements of both are necessary for site characterization.

The effects of atmospheric opacity and instability, important at all millimeter and submillimeter wavelengths, become more severe at higher frequencies. Observations at longer millimeter wavelengths, say > 2 mm, are practical at a relatively large number of sites, including established observatories and major cities. For observations at shorter wavelengths, especially in the submillimeter, the atmospheric limitations become so severe acceptable observing conditions are only found at a handful of sites worldwide.

2. Transparency

Atmospheric transparency is *the* fundamental site characteristic. Astronomical observations will be futile if cosmic radiation cannot penetrate the atmosphere. Unlike the situation with atmospheric stability, no (obvious) countermeasures are available to improve the intrinsic transparency of the atmosphere over a site.

Atmospheric opacity imposes a twofold penalty. “The degradation in [system] noise temperature due to *absorptive elements* results from two effects: reduction in signal . . . by . . . absorption and introduction of noise by re-radiation. . .” (Penzias & Burrus 1973). Moreover, the necessary integration time for sensitivity limited observations is proportional to the square of the system noise. Hence even a small fractional improvement in transparency can yield a large improvement in observing efficiency, especially at submillimeter wavelengths.

Table 1. Effect of transparency on integration time

ν [GHz]	T_{rec} [K]	τ_1	τ_2	t_1/t_2
220	55	0.05	0.04	1.1
345	83	0.17	0.14	1.2
675	162	1.10	0.88	1.8
875	210	1.21	0.97	1.8

Notes: Optical depth regressions [$\tau(\nu) = a(\nu)\tau_{220} + b(\nu)$] from Matsushita et al. 2000; ALMA receiver goals, $T_{\text{rec}} = 5h\nu/k$; median ambient air temperature at Chajnantor, $T_{\text{atm}} = 270$ K; first quartile zenith optical depth at Chajnantor, $\tau_2(225 \text{ GHz}) = 0.04$, and 25% degradation, $(\tau_1 - \tau_2)/\tau_2 = 0.25$; zenith observations, $A = 1$.

Consider sensitivity limited observations at different frequencies. The required integration time, t , depends on the square of the system noise, T_{sys} ,

$$t \propto T_{\text{sys}}^2 = e^{2\tau A} \left[T_{\text{rec}} + T_{\text{atm}} (1 - e^{-\tau A}) \right]^2, \quad (1)$$

where τ is the atmospheric optical depth at the zenith, T_{rec} is the receiver temperature, T_{atm} is the effective atmospheric radiation temperature, and $A = \sec(z)$ is the airmass at zenith angle z . (Secondary effects, including ground spillover and the cosmic background radiation, have been neglected.) Then to reach the same sensitivity in observations under two conditions, τ_1 and τ_2 , the ratio of the required integration times

$$t_1/t_2 = (T_{\text{sys},1}/T_{\text{sys},2})^2 \quad (2)$$

$$= e^{2(\tau_1 - \tau_2)A} \left[\frac{T_{\text{rec}} + T_{\text{atm}} (1 - e^{-\tau_1 A})}{T_{\text{rec}} + T_{\text{atm}} (1 - e^{-\tau_2 A})} \right]^2. \quad (3)$$

For example, a 25% degradation from the first quartile 225 GHz optical depth measured at Chajnantor implies an 80% penalty in observing time for zenith observations at submillimeter wavelengths (Table 1).

2.1. Atmospheric Spectrum

At millimeter and submillimeter wavelengths, the atmospheric spectrum is dominated by strong resonant absorption lines of the major molecular species, notably H_2O , O_2 , and O_3 . In addition, a pseudo-continuum with both wet and dry components contributes to atmospheric absorption. This pseudo-continuum, representing the far wings of very strong infrared lines, is stronger at higher frequencies. Models of the atmospheric spectrum were first presented by Van Vleck (1947a & b) and subsequently developed by many investigators. The latest ATM model (Pardo 2001; Pardo et al. 2001) largely supersedes earlier work. These models depend on the barometric pressure, or equivalently the site altitude, and

the temperature and water vapor profiles. Often the shape of the profiles can be assumed, so values of the surface temperature and the total precipitable water vapor are sufficient.

2.2. Tipping radiometers

Tipping radiometers are the primary tools for monitoring atmospheric transparency. Both continuum and line radiometers are in use. Continuum radiometers, either narrow or broad band, measure the total atmospheric opacity, including all components, directly at the wavelength of astronomical interest. Hence observing conditions can be assessed without recourse to a model. Conditions at other wavelengths must be estimated with a model. Line radiometers, on the other hand, measure the strength of an atmospheric emission line, usually either the 22 GHz or the 183 GHz water vapor line. The transparency is then inferred from an atmospheric model. Other components may not be measured.

Microwave sounding of the atmosphere was pioneered by Dicke et al. (1946), who determined the frequency and absorption coefficient of the 22.2 GHz water vapor line with a three-channel tipping radiometer. Their procedure, to “measur[e] the thermal radiation . . . emitted by the absorbing atmosphere. . . for the zenith direction and at several angles . . . from the vertical,” remains in use essentially unchanged.

By the early 1970s, tipping measurements became standard practice at millimeter telescopes for calibration (Penzias & Burrus 1973). In the meantime, meteorologists developed specialized radiometers for atmospheric sounding (Janssen 1993). Now, 220/225 GHz tippers have become a de facto standard for site characterization, deployed at many sites worldwide.

2.3. Transparency at Chajnantor, Mauna Kea, and the South Pole

Three premier sites for millimeter and submillimeter wavelength astronomy are Mauna Kea, the South Pole, and the ALMA site near Cerro Chajnantor, Chile. Measurements of the atmospheric transparency at both 225 GHz and 350 μm have been carried out with functionally identical tippers at all three sites to gauge observing conditions.

225 GHz measurements In the mid-1980s, NRAO constructed several heterodyne tipping radiometers to characterize observing conditions at sites under consideration for the Millimeter Array project (McKinnon 1987, Liu 1987). These instruments determine the atmospheric transparency at 225 GHz every 10 minutes. Although different computers and software have been used to control the tippers at different sites, the radiometers are functionally identical and the measurements are directly comparable (Radford & Chamberlin 2000).

One tipper has been in service at the Caltech Submillimeter Observatory on Mauna Kea (4100 m altitude) since 1989 August with only brief interruptions. Another tipper was deployed to the South Pole (2835 m) in 1992 (Chamberlin & Bally 1994, 1995). Since 1995 April, NRAO has operated a radiometer at the ALMA site (5060 m) near Cerro Chajnantor, Chile (Radford & Holdaway 1998).

It comes as no surprise that all three sites have periods of excellent observing conditions. Significant differences are apparent, however, in the cumulative distributions of the measured 225 GHz zenith optical depths, τ_{225} (Figure 1).

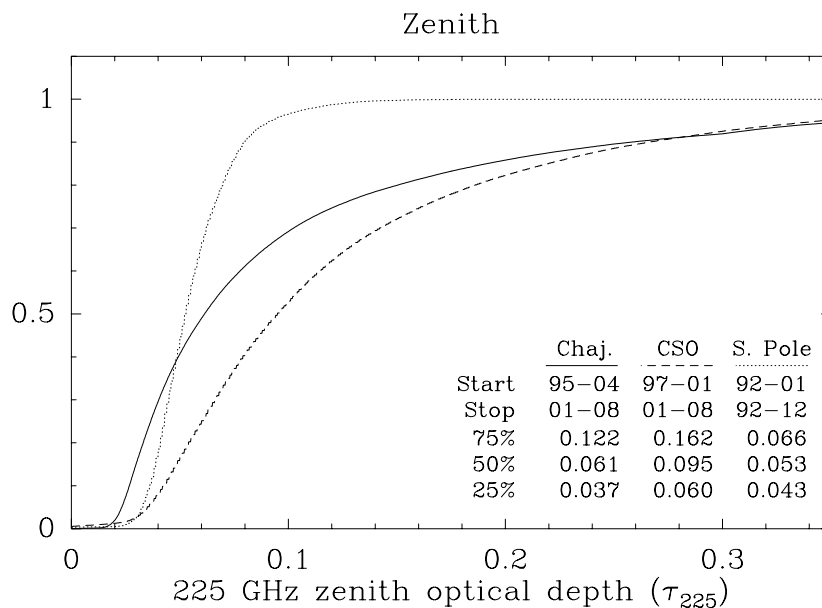


Figure 1. Cumulative distributions of the 225 GHz zenith optical depths (τ_{225}) measured at Chajnantor, at Mauna Kea (CSO), and at the South Pole. Adapted from Radford & Chamberlin (2000) with South Pole data taken from Chamberlin & Bally (1994, 1995).

Chajnantor and the South Pole both enjoy better conditions more often than Mauna Kea. The comparison between Chajnantor and the South Pole is more complex. The distributions cross near the fortieth percentile. During the best conditions at Chajnantor, the transparency is better than during the best conditions at the South Pole. The distribution at the South Pole, however, is far sharper than at the other sites.

There are significant seasonal variations at all three sites, with winters better than summers (Figure 2). At Chajnantor, conditions are consistently good from April through December but deteriorate during January, February, and March. In northern Chile, the summer months are known paradoxically as the “Bolivian winter” because a shift in the atmospheric circulation patterns draws moist air over the Andes from the Amazon basin. There is considerable year-to-year variation in the severity of this summer season. Nevertheless, even during the worst months on record, the median 225 GHz optical depth at Chajnantor, $\tau_{225} \approx 0.3$, is comparable to good conditions at many established observatories for millimeter wavelength astronomy. The seasonal pattern for Mauna Kea, although obvious, is overshadowed by the year-to-year variations. At the South Pole, the transparency during the cold, dark winter is substantially better than during the sunlit summer.

Both Chajnantor and Mauna Kea experience diurnal transparency variations, with better conditions at night (Figure 3). At both places, these diurnal transparency variations lag behind the solar cycle. The best conditions occur around sunrise at Chajnantor and a few hours after midnight at Mauna Kea.

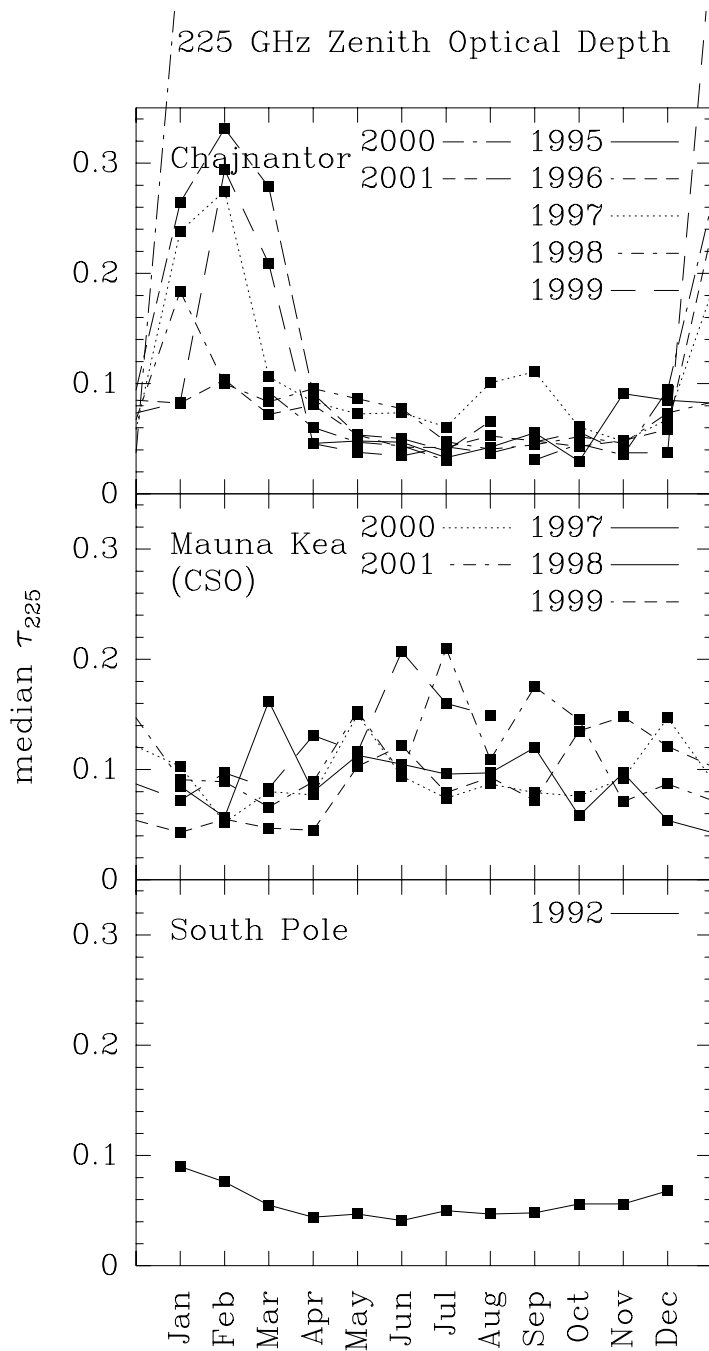


Figure 2. Seasonal variation of median measured broadband 225 GHz zenith optical depths at Chajnantor (*top*), Mauna Kea (CSO; *center*), and the South Pole (*bottom*). South Pole data taken from Chamberlin & Bally (1994, 1995).

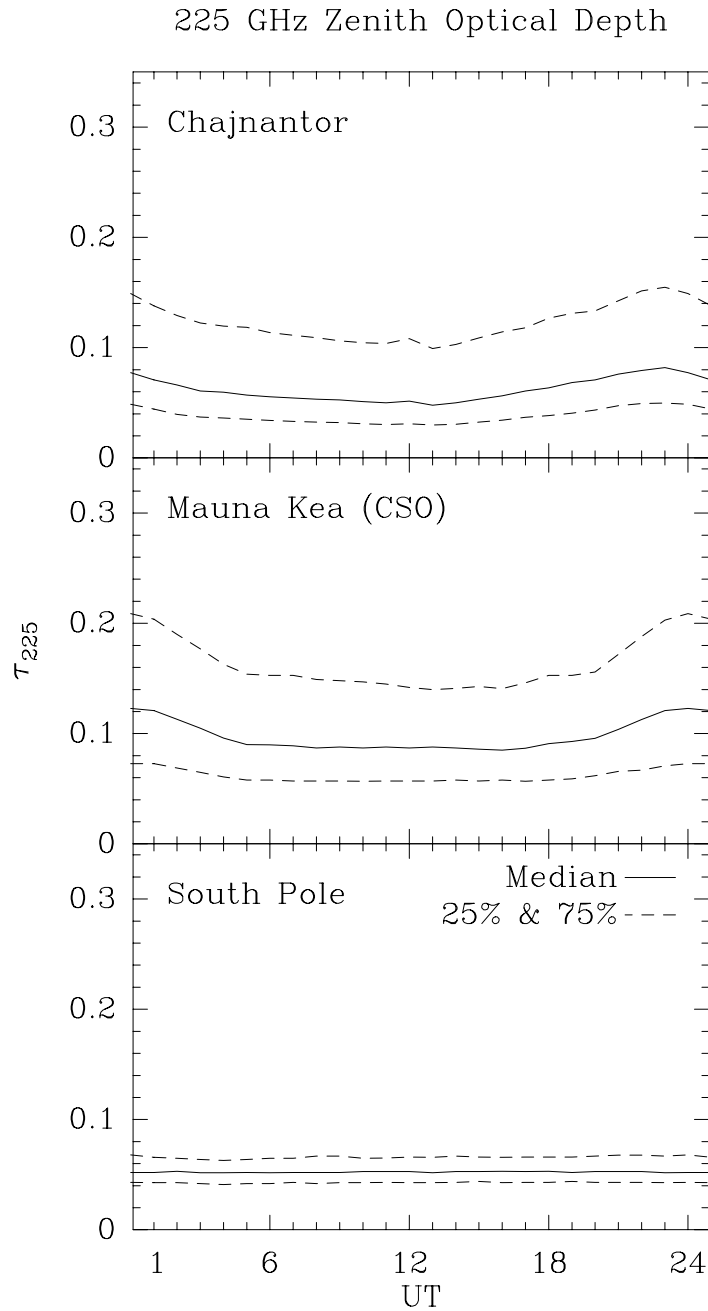


Figure 3. Diurnal variation of quartiles of measured broadband 225 GHz zenith optical depths at Chajnantor (*top*), Mauna Kea (CSO; *center*), and the South Pole (*bottom*). Local solar time is UT $- 4^{\text{h}} 30^{\text{m}}$ at Chajnantor and UT $- 10^{\text{h}} 22^{\text{m}}$ at Mauna Kea. South Pole data taken from Chamberlin & Bally (1994, 1995).

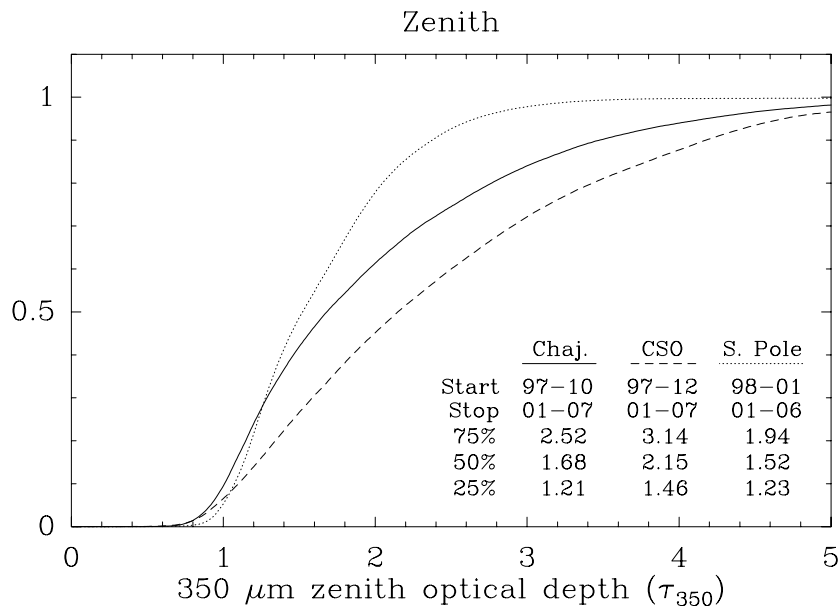


Figure 4. Cumulative distributions of the $350\ \mu\text{m}$ zenith optical depth (τ_{350}) measured at Chajnantor, at Mauna Kea (CSO), and at the South Pole.

At Chajnantor, the diurnal variations are weaker during the winter than during the summer. No 24 h cycle is apparent in the data for the South Pole, where the diurnal and seasonal cycles are congruent.

350 μm measurements Enticed by the scientific interest in high frequency observations but concerned by uncertainties inherent in extrapolating from the low 225 GHz optical depths measured at Chajnantor and at the South Pole, the NRAO and Carnegie Mellon University together developed a tipper to directly measure the atmospheric transparency at $350\ \mu\text{m}$ wavelength (Radford et al. 2002). This instrument is based on an ambient temperature, pyroelectric detector. A compound parabolic (Winston) cone and offset parabolic scanning mirror together define the 6° beam on the sky. The detector is internally calibrated with two temperature controlled loads and views the sky through a woven Gore-tex window. The instrument passband, defined by a resonant metal mesh filter, is matched to the $350\ \mu\text{m}$ atmospheric window. Because the instrument averages the sky brightness over this window, the measured transparency is less than the peak transparency at frequencies near the center of the window. Identical instruments are deployed on Chajnantor (1997 October), on Mauna Kea beside the CSO (1997 December), and at the South Pole (1998 January).

The $350\ \mu\text{m}$ measurements (Figure 4) show the atmosphere will be a limiting factor for submillimeter astronomy. Even under the best conditions at these excellent sites, the atmospheric terms are the predominant contributions to the system noise (Equation 1).

Qualitative extrapolations of conditions for high frequency observations from 225 GHz measurements are justified. The distributions of the measured 350 μm optical depths (Figure 4) are similar to the distributions of the 225 GHz measurements (Figure 1). The first quartile 350 μm transparencies at Chajnantor and the South Pole are roughly equal and noticeably better than at Mauna Kea. Quantitative extrapolation, on the other hand, depends on the temperature and pressure and must be evaluated for each site individually.

At 350 μm , the seasonal and diurnal variations (Figures 5 & 6) are also similar to the analogous characteristics of the 225 GHz measurements (Figures 2 & 3). Winter conditions at Chajnantor show less inter-annual variability than at Mauna Kea. Conditions at the South Pole, especially during the winters, show remarkable year-to-year consistency.

2.4. Line radiometers

Line radiometers recover the amount, and sometimes the vertical distribution, of an atmospheric component by measuring the strength of an emission line (e. g., Janssen 1993). The 22 GHz line is widely used by meteorologists for monitoring water vapor, the 60 GHz oxygen complex is used to recover the temperature profile, and the 183 GHz water vapor line is used for water vapor under low humidity conditions. Although these instruments have been used for site characterization (e. g., Delgado et al. 1999), their principle radioastronomy application has been for phase correction and calibration (e. g., Woody 2001).

2.5. Radiosondes

Radiosonde soundings provide direct measurements of the water vapor profile and other atmospheric parameters. The atmospheric transparency can then be evaluated from these data and a spectral model. This approach is subject, however, not only to uncertainties in the spectral model, but also to uncertainties in the performance of the radiosonde sensors, especially under the conditions of low humidity or low temperature that are most interesting for submillimeter astronomy. Because of the logistical requirements, radiosonde launches are relatively infrequent, at most a few times per day. Nevertheless, historical records often extend for many years, so radiosonde data are a valuable resource for long term climate monitoring (Bustos et al. 2000; Chamberlin 2001a, b).

2.6. Spectroscopy

Tipping radiometers are relatively simple instruments with modest support requirements, so they are good for long term site monitoring. But typically they measure the atmospheric transparency for only a single wavelength (or broadband window). Wide band spectrometers, on the other hand, are complex and usually require cryogenic cooling, but they provide detailed atmospheric spectra for comparison with models. Fourier transform spectrometers covering submillimeter wavelengths have been deployed recently on Mauna Kea at the CSO (Serabyn et al. 1998; Pardo et al. 2001a; Serabyn 2001), in northern Chile at Pampa la Bola (Matsuo et al. 1998; Matsushita et al. 1999, 2000) and at Chajnantor (Paine et al. 2000), and at the South Pole (Chamberlin private comm.).

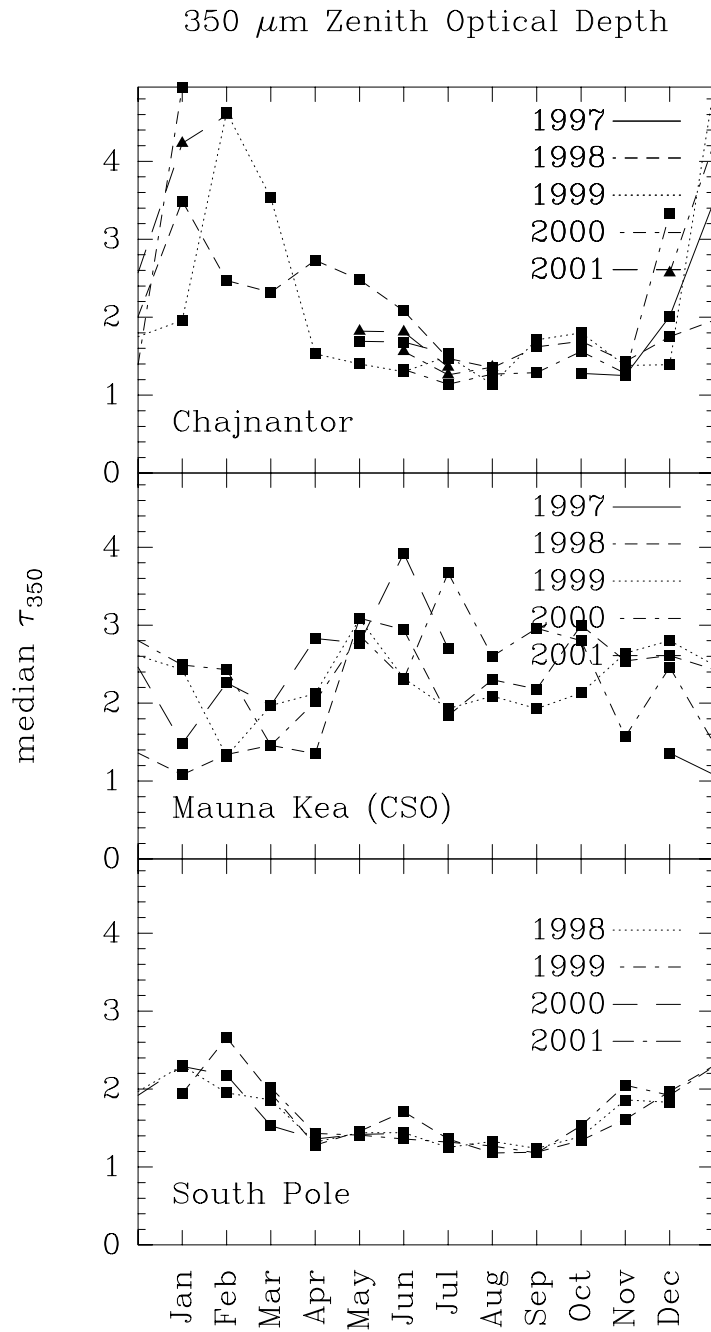


Figure 5. Seasonal variation of median measured broadband 350 μm zenith optical depths at Chajnantor (*top*), Mauna Kea (CSO; *center*), and the South Pole (*bottom*).

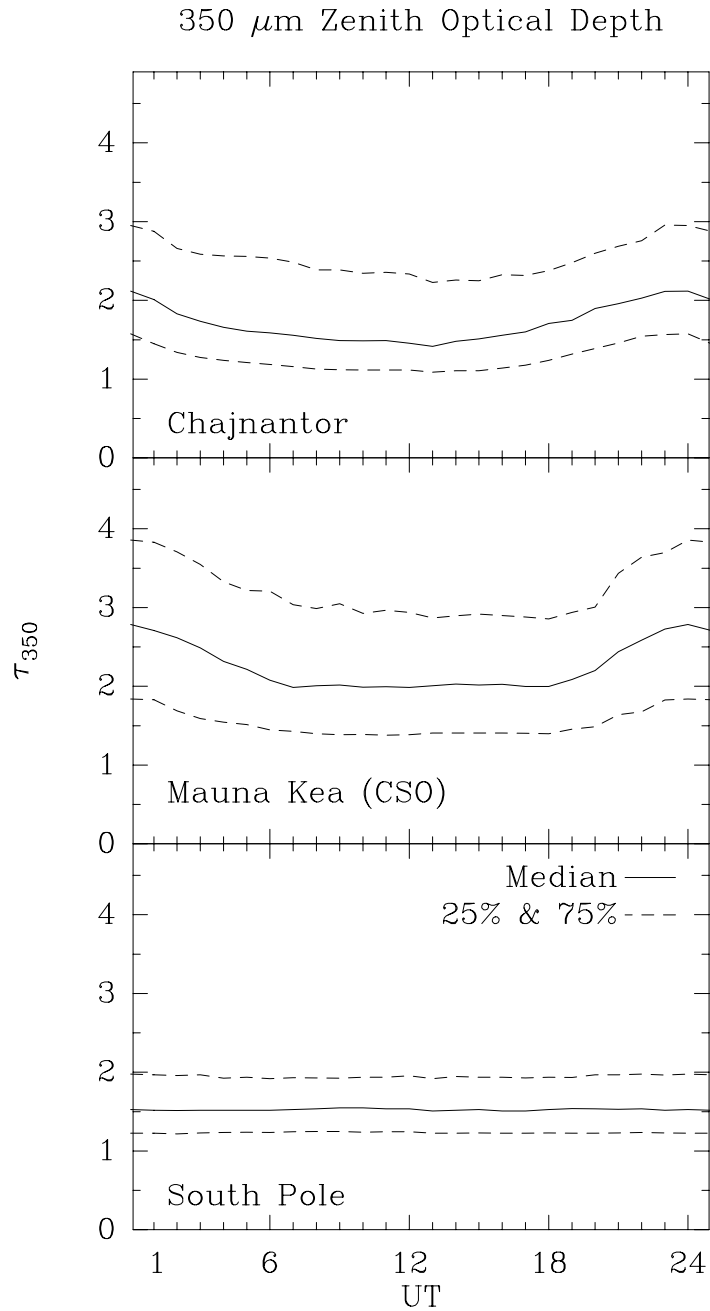


Figure 6. Diurnal variation of quartiles of measured broadband 350 μm zenith optical depths at Chajnantor (*top*), Mauna Kea (CSO; *center*), and the South Pole (*bottom*). Local solar time is UT $- 4^{\text{h}} 30^{\text{m}}$ at Chajnantor and UT $- 10^{\text{h}} 22^{\text{m}}$ at Mauna Kea.

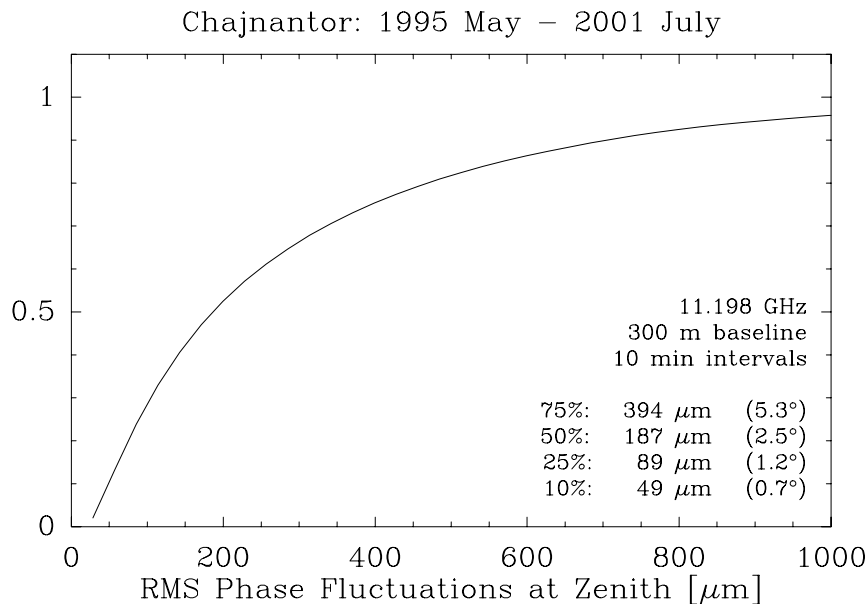


Figure 7. Cumulative distribution of ϕ_{rms} , the r. m. s. phase fluctuations measured at Chajnantor on a 300 m baseline at 11.198 GHz and referenced to the zenith.

3. Stability

The effects of atmospheric instability on radio observations were initially recognized in late 1960s at cm interferometers (e. g., Hinder & Ryle 1971; Baldwin & Wang 1989). Because radio waves travel more slowly through wet air than through dry air, fluctuations in the water vapor content cause variations in the electrical path length through the atmosphere. For an interferometer array, path length differences between array elements will degrade both the array sensitivity, by decorrelating the signals on short time scales, and the image quality, by introducing phase errors on long time scales that broaden the synthesized beam. For an individual telescope, phase gradients across the aperture change the effective telescope pointing, reducing the calibration fidelity.

Atmospheric stability is not, however, as fundamental a site characteristic as transparency because there are schemes for ameliorating the effects of atmospheric fluctuations (e. g., Woody 2001).

3.1. Test Interferometers

Atmospheric stability can be measured directly from the phase fluctuations seen by a simple interferometer observing a convenient beacon outside the atmosphere, i. e., on a geostationary satellite. This technique was pioneered by Ishiguro et al. (1990), who observed a 19.45 GHz beacon over a single 35 m baseline. They demonstrated a good correlation between the phase fluctuations measured with their test interferometer and those measured on similar baselines at 98 GHz during simultaneous observations of 3C 273. Subsequently, site characterization

Table 2. Chajnantor phase stability

	measured ϕ_{rms}		ν_{limit} [GHz]	
	[μm]	[$^{\circ}$]	30°	70°
75 %	394	5.3°	63	148
50 %	187	2.5°	134	313
25 %	89	1.2°	281	655
10 %	49	0.7°	510	1189

ϕ_{rms} : r. m. s. fluctuations on a 300 m baseline at 11.198 GHz at 36° elevation over 10 min intervals referenced to the zenith. ν_{limit} : frequency limit for observations with specified r. m. s. phase fluctuations.

interferometers with 100–300 m baselines have been developed and deployed by the SAO (Masson 1994), the NRAO (Radford, Reiland, & Shillue 1996), and the BIMA (Lay 1998). The NRO, SAO, and NRAO instruments all observe monochromatic beacons, while the BIMA instrument has a novel design employing analog multipliers to observe wide band television broadcast signals. Because the atmosphere is (largely) non-dispersive away from line centers, low frequency measurements can be extrapolated to characterize the atmospheric phase stability at least up to 350 GHz.

At Chajnantor, the atmospheric phase stability at 11.2 GHz is monitored continuously over a 300 m, east-west baseline. The interferometer phase is measured every second and the r. m. s. phase fluctuations calculated for 10 min intervals after quadratic trends are subtracted to allow for satellite libration and slow drifts in the intrinsic instrument phase. This interval is thirty times longer than it takes for atmospheric features to travel the baseline length at 10 m s^{-1} , a typical wind speed aloft. Because the satellite elevation is 36° , the measurements have been scaled to the zenith by $(\sec z)^{1/2}$, which is appropriate for baselines less than the thickness of the turbulent layer. (Holdaway et al. 1995).

In interferometric observations, phase decorrelation reduces the sensitivity by $\exp(-\phi_{\text{rms}}^2/2)$, where ϕ_{rms} is the r. m. s. phase fluctuation level in radians. (Thompson, Moran, & Swenson 2001). Phase fluctuations less than 10° r. m. s. have little impact upon most imaging, fluctuations of 30° r. m. s. permit 200:1 dynamic range imaging, but impose a 13% sensitivity loss, and image reconstruction becomes all but impossible and the observing time penalty becomes excessive for fluctuations greater than 70° r. m. s. (Holdaway and Owen 1995).

Scaling the 11.2 GHz phase fluctuations measured at Chajnantor (Figure 7) allows an estimate of the highest frequency where phase stable observations are possible (Table 2). On 300 m baselines, which are modest for the ALMA, compensation for atmospheric phase fluctuations will be necessary much of the time at millimeter wavelengths and most of the time at submillimeter wavelengths.

At both Mauna Kea and Chajnantor, the phase stability is better in winter, the diurnal phase stability variation is larger than the seasonal variation, and the diurnal variation is more pronounced in phase stability than in transparency (Masson 1994; Radford & Holdaway 1998). At Chajnantor, the diurnal

phase stability variation more nearly matches the solar cycle than the diurnal transparency variation.

3.2. Brightness fluctuations

Inhomogeneities in the atmospheric water vapor distribution also produce fluctuations in the sky brightness. In the context of site characterization, brightness fluctuations have been discussed by McKinnon (1988) and Foster, Holdaway, and Owen (1996) for interferometers, by Lay and Halverson (1999) for observations of the Cosmic Background Radiation, and by O’Kelly et al. (2002) for submillimeter astronomy.

4. Transparency and Stability

Comprehensive site characterization requires measurements of both atmospheric transparency and stability. In general, these quantities appear only poorly correlated (Figure 8; Masson 1994). All combinations of transparency and stability are observed. This suggests only a small fraction of the total water vapor column participates in the turbulence leading to path length fluctuations.

Acknowledgments. It’s a pleasure to thank Bryan Butler, Angel Otárola, Mark Holdaway, Jeff Mangum, Lars-Åke Nyman, Guillermo Delgado, Jeff Peterson, Ethan Schartman, Virginia Valentine, Richard Chamberlin, Scott Paine, Ray Blundell, Seiihi Sakamoto, Juan Pardo, Satoki Matsushita, H. Matsuo, Gerardo Valladares, Frazer Owen, Gerry Petencin, for collaboration, conversation, and advice. The National Radio Astronomy Observatory is a facility of the National Science Foundation operated under cooperative agreement by Associated Universities, Inc.

References

- Baldwin, J. E., & Wang S. 1990, Radio Astronomical Seeing (Beijing: IAP)
- Bustos, R., Delgado, G., Nyman, L.-Å., & Radford, S. 2000, ALMA Memo 333 (NRAO)
- Chamberlin, R. A. 2001a, JGR Atmospheres in press
- Chamberlin, R. A. 2001b, these proceedings
- Chamberlin, R. A., & Bally, J. 1994, Appl. Opt. 33, 1095
- Chamberlin, R. A., & Bally, J. 1995, Int. J. IR MM Waves 16, 907
- Delgado, G., Otárola, A., Belitsky, V., Urbain, D., Hills, R., & Martin-Cocher, P. 1999, ALMA Memo 271.1 (NRAO)
- Dicke, R. H., Beringer, R., Kyhl, R. L., & Vane, A. B. 1946, Phys. Rev. 70, 340
- Foster, S. M., Holdaway, M. A., & Owen, F. N. 1996, National Radio Science Meeting (Washington, D. C.: National Academy of Sciences) p. 235
- Holdaway, M. A., Radford, S. J. E., Owen, F. N., & Foster, S. M. 1995, MMA Memo 129 (NRAO)
- Holdaway, M. A., & Owen, F. N. 1995, MMA Memo 136 (NRAO)

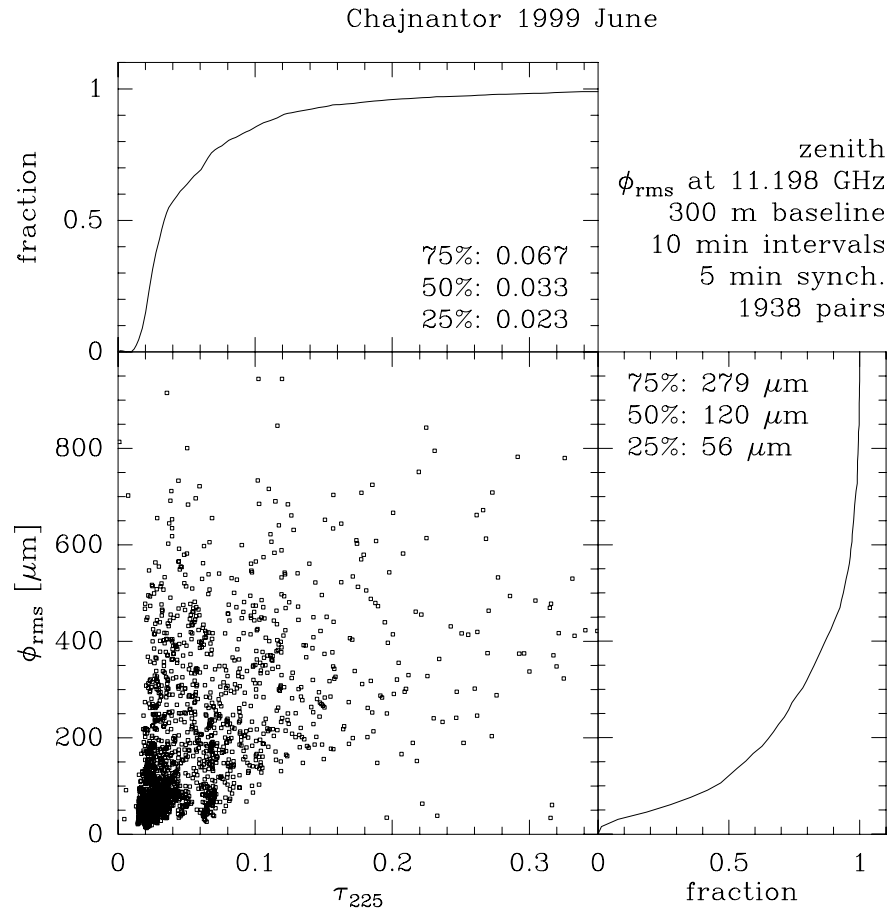


Figure 8. Simultaneous measurements at Chajnantor during 1999 June of τ_{225} , the 225 GHz zenith optical depth, and of ϕ_{rms} , the r. m. s. phase fluctuations on a 300 m baseline at 11.198 GHz and referenced to the zenith.

- Holdaway, M. A., Ishiguro, M., Nakai, N., & Matsushita, S. 1996, MMA Memo 158 (NRAO)
- Hinder, R., & Ryle, M. 1971, MNRAS 154, 229
- Ishiguro, M., Kanzawa, T., & Kasuga T. 1990, in Radio Astronomical Seeing, eds. Baldwin, J. E., & Wang S. (Beijing: IAP) p. 60
- Janssen, M. A. 1993, Atmospheric Remote Sensing by Microwave Radiometry, (New York: Wiley)
- Lay, O. 1999, BIMA Tech Memo 72 (U. C. Berkeley)
- Lay, O. P., & Halverson, N. W. 2000, ApJ 543, 787
- Liu, Z.-Y. 1987, MMA Memo 41 (NRAO)
- Masson, C. R., 1994, in IAU Colloq. 140: Astronomy with Millimeter and Submillimeter Wave Interferometry, ed. Ishiguro, M., & Welch, W. J. (San Francisco: ASP) p. 87
- Matsuo, H., Sakamoto, A., & Matsushita, S. 1998, PASJ 50, 359
- Matsushita, S., Matsuo, H., Pardo, J. R., & Radford, S. J. E. 1999, PASJ 51, 603
- Matsushita, S., Matsuo, H., Sakamoto, A., & Pardo, J. R. 2000, Proc. SPIE 4015, 378
- McKinnon, M. 1987, MMA Memo 40 (NRAO)
- McKinnon, M. 1988, MMA Memo 49 (NRAO)
- O’Kelly, M. J., Peterson, J. P., Radford, S. J. E., Schartman, E., Chamberlin, R. A., & Ade, P. A. R. 2002, in preparation
- Paine, S., Blundell, R., Papa, D. C., Barrett, J. W., Radford, S. J. E. 2000, PASP 112, 108
- Pardo, J. R. 2001, these proceedings
- Pardo, J. R., Serabyn, E., & Cernicharo, J. 2001a, J. Quant. Spec. Rad. Transfer 68, 419
- Pardo, J. R., Cernicharo, J., & Serabyn, E. 2001b, IEEE Trans. Ant. Prop. in press
- Penzias, A. A., & Burrus, C. A. 1973, ARAA 11, 51
- Radford, S. J. E., & Chamberlin, R. A. 2000, ALMA Memo 334.1 (NRAO)
- Radford, S. J. E., & Holdaway, M. A. 1998, Proc. SPIE 3357, 486
- Radford, S. J. E., Peterson, J. P., Schartman, E., Valentine, V., & Chamberlin, R. A. 2002, in preparation
- Radford, S. J. E., Reiland, G., Shillue, B. 1996, PASP 108, 441
- Serabyn, E., Weisstein, E. W., Lis, D. C., & Pardo, J. R. 1998, Appl. Opt. 37, 2185
- Serabyn, E. 2001, these proceedings
- Thompson, A. R., Moran, J. M., & Swenson, G. W., Jr. 2001, Interferometry and Synthesis in Radio Astronomy, 2nd ed. (New York: Wiley)
- Van Vleck, J. H. 1947a, Phys. Rev. 71, 413
- Van Vleck, J. H. 1947b, Phys. Rev. 71, 425
- Woody, D. 2001, these proceedings